UC San Diego
Oceanography Program Publications

Title
A Comparison of Spectral Refraction and Refraction-Diffraction Wave Models

Permalink
https://escholarship.org/uc/item/3ds995nm

Journal
Journal of Waterway Port, Coastal and Ocean Engineering, 117(3)

Authors
O'Reilly, W C
Guza, R T

Publication Date
1991-05-01

Data Availability
The data associated with this publication are available upon request.

Peer reviewed

eScholarship.org Powered by the California Digital Library
University of California

COMPARISON OF SPECTRAL REFRACTION AND REFRACTION-DIFFRACTION WAVE MODELS

By W. C. O'Reilly,[1] Member, ASCE, and R. T. Guza[2]

ABSTRACT: Wave energy estimated from linear, spectral wave propagation models incorporating refraction and refraction-diffraction are compared over two bottom configurations: an analytic circular shoal and relatively smooth coastal bathymetry from San Diego, California. The agreement between the two models improves with an increase in the width of the incident directional spectrum and with a decrease in the complexity of the local bathymetry. There are, however, significant differences between the model transformations of directionally narrow spectra on both bathymetries. Pure refraction models are not quantitatively accurate in these cases. These comparisons also demonstrate the importance of directional wave spreading in transformations over even relatively simple natural bathymetry. Data from a fundamentally low-resolution pitch-and-roll buoy, if used as the sole source of directional information for incident waves, can lead to significant uncertainty in wave heights estimated by the refraction-diffraction model.

INTRODUCTION

The need for accurate surface gravity wave information has recently led to a rapid development of wave modeling techniques. In addition, the advent of microcomputers has eliminated the necessity of a number of simplifications concerning wave transformations in shallow water. One of the most questionable model simplifications is the reduction of an incident wave frequency-directional spectrum into a few wave trains. Vincent and Briggs (1989) showed that wave transformations over a laboratory shoal are sensitive to the shape of the incident wave directional spectrum and differ significantly from a single unidirectional wave. The representation of a wave field as a spectrum is not new, but has only recently become commonplace in engineering practice [e.g., Goda (1985) and others].

Wave transformation models that include refraction and diffraction have progressed dramatically since Radder (1979) applied the parabolic equation method (PEM) to the mild-slope equation (Berkhoff 1972). Kirby (1986a,b) describes higher-order approximations in PEM methods, which permit wave propagation at larger angles to the principle wave direction. Typically, solutions of the mild-slope equation are obtained for incident waves of a single frequency and direction, or a combination of phase-locked waves with a single frequency and multiple directions. Isobe (1987), Izumiya and Horikawa (1987), and Panchang et al. (1990) have applied PEM models to the transformation of incident wave frequency-directional spectra by combining multiple model runs, each for a single frequency and direction. These spectral models do not explicitly predict the directional spectrum, but have been used to estimate the directionally integrated energy (i.e., wave height). Finally, a very wide-angle refraction-diffraction model, which allows for the

[1]Res. Asst., Ctr. for Coastal Studies, Scripps Instn. of Oceanography, La Jolla, CA 92093.

[2]Prof., Ctr. for Coastal Studies, Scripps Instn. of Oceanography, La Jolla, CA.

Note. Discussion open until October 1, 1991. To extend the closing date one month, a written request must be filed with the ASCE Manager of Journals. The manuscript for this paper was submitted for review and possible publication on June 16, 1990. This paper is part of the ***Journal of Waterway, Port, Coastal, and Ocean Engineering***, Vol. 117, No. 3, May/June, 1991. ©ASCE, ISSN 0733-950X/91/0003-0199/$1.00 + $.15 per page. Paper No. 25795.

evolution and propagation of directional "modes" from a single incident wave direction, has recently been developed by Dalrymple and Kirby (1988) and Dalrymple et al. (1989). The high-order PEM (Padé approximant) method (Kirby 1986a) is used here.

The theory of wave spectra transformations by refraction was first proposed by Pierson et al. (1953), later theoretically derived by Longuet-Higgins (1957), and discussed more recently by LeMehaute and Wang (1982). The transformed directional spectrum is estimated from the incident wave spectrum by back-refracting rays from the target site.

This paper compares wave energy predictions from a linear spectral refraction (R) model with the linear form of a spectral PEM refraction-diffraction (RD) model [extended for wave spectra as described by Isobe (1987) and Izumiya and Horikawa (1987)]. The R model can be very efficient numerically when the incident waves propagate over a large area, and transforms the directional portion of the wave spectrum in a more straightforward manner. Conditions under which the methods yield comparable results are therefore of practical interest.

The RD and R models are first briefly reviewed. Wave energy estimates by the two models are compared for broad and narrow incident directional spectra on an analytic circular shoal, and a relatively featureless coastline near Mission Beach, California. Although the model results are similar with broad directional spectra, they differ significantly with a narrow directional spread. Thus, diffraction can be important even on relatively smooth natural bathymetry. Finally, we show that the directional sensitivity of wave transformations is such that field testing of RD models may be limited by the accuracy of the estimated incident directional spectra.

Spectral Transformations by Refraction and Diffraction

The refraction-diffraction model used here is based on the linear version of the higher-order PEM derived by Kirby (1986a) and discussed further in Kirby (1986c), and Kirby and Dalrymple (1986). Berkhoff (1982) and Kirby (1986a) have compared a unidirectional PEM refraction-diffraction model, and Panchang et al. (1990) a spectral PEM refraction-diffraction model, with laboratory data for waves propagating over a shoal. The models predicted the transformed wave heights quite well. For unidirectional waves, the weakly nonlinear form of the unidirectional refraction-diffraction model compared more favorably with laboratory measurements than the linear model. However, a nonlinear spectral model requires individual model runs over the range of possible initial wave energies as well as frequencies and directions. These additional model runs are computationally intensive, and the present discussion is limited to linear models.

Izumiya and Horikawa (1987) used a PEM model to transform a directional wave spectrum over parallel contours, where there is a one-to-one relationship between the incident and transformed wave directions. The single transformed wave direction is calculated from the phase difference between the solutions at two neighboring points on the numerical grid. Directional transformations are more complicated over irregular bathymetry, since a single incident direction (and frequency) can be transformed into multiple directions. In these cases, the RD solutions describe a partially standing transformed wave field resulting from the interference of phase-locked waves

with the same frequency, but propagating from multiple directions. Using the grid points as an array of wave gauges to resolve the directional components of a spatially inhomogeneous, partially standing wave field, is markedly more complicated than estimating the directional spectrum of a spatially homogeneous wave field, and was not attempted here. Instead, solutions at the RD-model grid points were used to estimate directionally integrated wave energies. In the examples that follow, the incident directional spectra are transformed at a single wave frequency of 0.06 Hz. The incident wave directional spectrum is discretized with a uniform directional bandwidth. The transformed, directionally integrated energy is the sum of the contributions from each of these input directions

$$E = \int S(\theta) d\theta \approx \sum_{i=1}^{N} \delta(\theta_{oi}) S_o(\theta_{oi}) \Delta\theta_{oi} \quad \ldots\ldots (1)$$

with δ defined as the ratio of transformed energy to incident energy, calculated from the RD model for each direction. The number of individual RD model runs, N, required to adequately define δ is bathymetry dependent. Since the RD model is linear, the response at each grid point need only be calculated once, for an incident wave of unit amplitude, at each frequency and direction. The response to any desired incident directional spectrum is then constructed by appropriately weighting each discrete component. This is the equivalent of assuming there is no phase coupling between the different directional components of the incident wave field. The extension to include frequency as well as directional spread in the incident wave field is straightforward.

Spectral Transformations by Refraction

If diffractive effects are neglected, the relationship between a spatially homogeneous incident wave spectrum, S_o, and a wave spectrum at a shallow-water or sheltered location, S, is given by

$$S(\omega, \theta) = \frac{k}{k_o} \frac{C_{go}}{C_g} S_0(\omega, \theta_o) \quad \ldots\ldots (2)$$

The subscript, o, refers to the incident wave spectrum; k = the wave number; and C_g = the group velocity for a given wave frequency and water depth.

Eq. 2 is valid along a ray path, and the relationship between θ and θ_o is obtained by back-refracting a directional range of rays from a specific location. LeMehaute and Wang (1982) refer to this relationship as the inverse direction function, Γ, where $\theta_o = \Gamma(\omega, \theta)$. Eq. 2 then becomes

$$S(\omega, \theta) = \frac{k}{k_o} \frac{C_{go}}{C_g} S_o[\omega, \Gamma(\omega, \theta)] \quad \ldots\ldots (3)$$

A sufficient number of rays must be back-refracted to adequately define Γ in frequency and directional space. The number of rays and their directional spacing depend on both the complexity of the bathymetry along with the frequency and directional scales over which the incident wave spectrum is approximately constant. This procedure is somewhat analogous to numerically integrating a function, with additional ray calculations performed where Γ varies most rapidly with ω and θ.

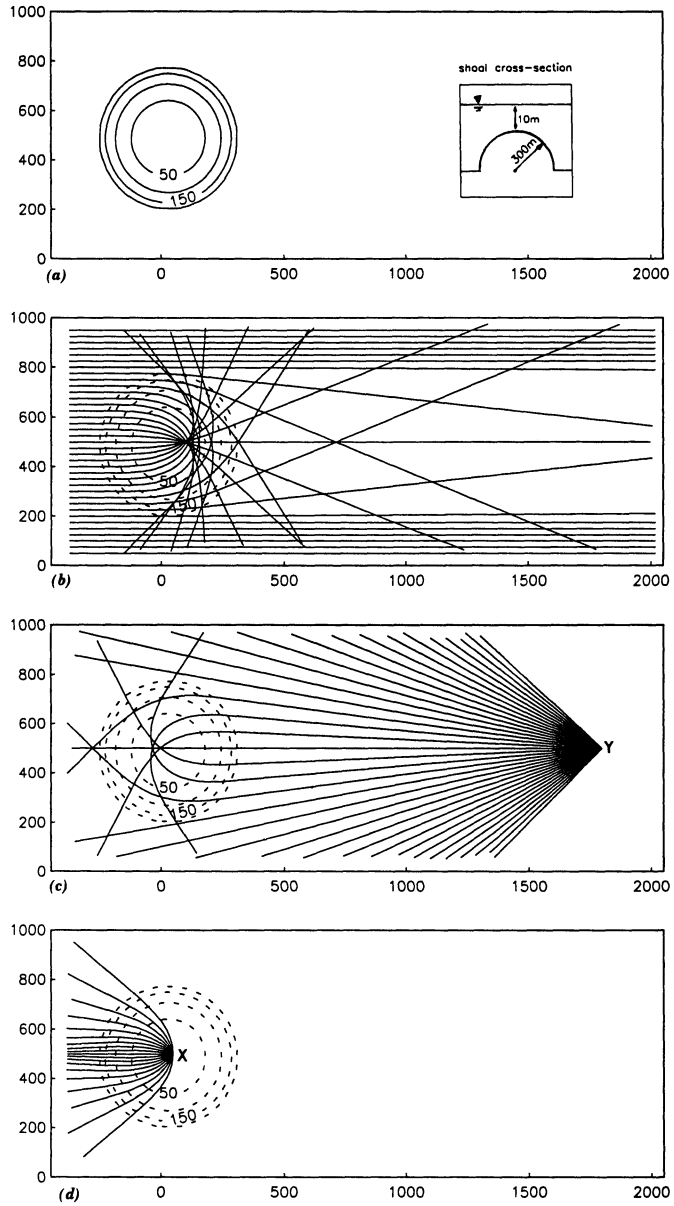

FIG. 1. Forward (Left to Right) and Back-Refracted Rays over Circular Shoal. Depth Contours and Axes are in Meters; Wave Frequency, f = 0.06 Hz: (*a*) Circular Shoal Configuration, Bottom Depth around Shoal = 310 m; (*b*) Forward-Refracted Waves, Initial Ray Spacing = 25 m, Initial Angle = 180°; (*c*) Back-Refracted Waves, Initial Angle Spacing = 2.5°; (*d*) Back-Refracted Rays, Initial Angle Spacing = 10°

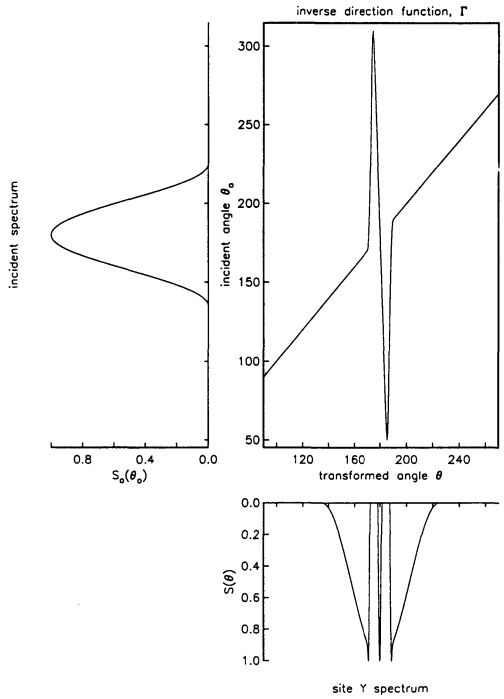

FIG. 2. Spectral Transformation of Arbitrarily Selected Incident (f = 0.06 Hz) Wave Directional Spectrum (Upper-Left Panel) to Location Y (Lower-Right Panel); kC_{go}/k_oC_g = 1. Units of Spectra are Arbitrary and Upper-Right Panel is Inverse Direction Function for Location Y in Fig. 1(*c*)

Refraction models based on the concept of a continuous directional spectrum are robust in comparison with traditional (nonspectral) ray theory, which will be referred to as forward ray tracing. These methods are fundamentally different; the caustics that plague forward ray tracing schemes do not occur in the spectral model. For example, when forward ray tracing is performed over a circular shoal [Fig. 1(*a*)], caustics, inidicated by the crossing of adjacent rays [Fig. 1(b)], result in infinite, or arbitrary, wave heights. In the spectral model, rays are back-refracted from site Y behind the shoal [Fig. 1(*c*)] to define the inverse direction function, Γ, (Fig. 2). Note that crossing rays created when back-refracting do not generally represent caustics since the rays are associated with different incident angles, θ_o. However, the local maxima or minima in Γ, where $\partial\theta_o/\partial\theta = 0$, indicate the incident directions from which forward-refracted rays would form a caustic point directly at Y. Eq. 3 can be used to transform an incident spectrum of any shape to a finite spectrum at site Y (demonstrated as a $\theta_o \rightarrow \theta$ mapping in Fig. 2).

It is interesting to examine how the caustics of unidirectional forward refraction theory are manifested in spectral refraction solutions. Back-refracted rays are shown for site X, 75 m down wave of the shoal center [Fig. 1(*d*)]. The transformation of incident energy from θ_{co} to θ_c at site X is shown in Fig. 3. These directions are associated with the local maxima in Γ. The

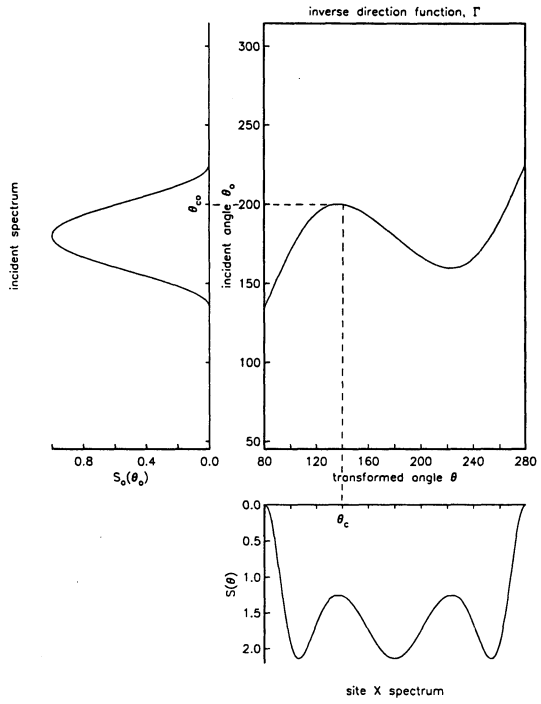

FIG. 3. Spectral Transformation of Incident Wave Spectrum to Location X in Fig. 1(*d*); $kC_{go}/k_oC_g = 2.14$. Same Format as Fig. 2. Incident Angle θ_{co} Produces Caustic at Transformed Angle θ_c

"caustic" energy at X is defined from Eq. 3, with $J = kC_{go}/k_oC_g = 2.14$, as

$$E_c = J \int_{\theta_c} S_o[\omega, \Gamma(\omega, \theta)] d\theta = JS_o(\omega, \theta_{co}) \int_{\theta_c} d\theta = JS_o(\omega, \theta_{co}) \Delta\theta_c \quad \ldots\ldots\ldots\ldots \quad (4)$$

where $\Delta\theta_c$ refers to the small range of continuous transformed directions that back-refract to the same incident direction, θ_{co}. Over this range of directions, the back-refracted rays are the same as the forward rays that form a caustic at site X. Thus, E_c is the total amount of wave energy contained between the rays that formed the caustic, now spread over a small range of transformed wave directions $\Delta\theta_c$. At the caustic point, the rays' finite energy density per unit wave-crest length is transformed to energy density per unit θ. Spectral refraction allows the finite energy associated with forward rays to pass through caustics, and continue to propagate as dictated by the rays. This is still a pure refraction problem, but the introduction of a directional spectrum yields finite wave amplitudes everywhere.

Unlike RD models applied to spectra, spectral R transformations are not the summation of a number of unidirectional (i.e., fundamentally nonspectral) solutions. The R model is directionally spectral throughout its derivation, and through its more moderate treatment of caustic forming bathym-

etry, it can provide useful wave energy estimates where the overall diffractive effects associated with an incident wave spectrum are small.

Spectral Transformations over Circular Shoal

The circular shoal [Fig. 1(*a*)] is used to explore the limitations of the spectral R model, which produced severe caustics with unidirectional refraction [Fig. 1(*b*)]. The transformed spectra are compared along the axis of the grid, at cross sections just down wave of the shoal where the wave field is evolving rapidly, and in the far field (Fig. 4).

Back-refraction for the R model was performed at individual points along the axis and cross sections with a wave frequency of $f = 0.06$ Hz, an angle step size of 0.1° and a grid spacing of 25 m. The RD model was run for incident angles from 135° to 225°, corresponding to ±45° from the x-axis (although the solution is symmetric about the axis). An incident angle step size of 1° was used with a grid spacing of 25 m. Two directional spectra were transformed, a very narrow spectrum with a full width at half maximum (FWHM) equal to 5°, and a broad spectrum with FWHM = 45° (Fig. 5).

In the narrow case (Fig. 6), the R model estimates a finite but unrealistically large wave energy maximum along the axis. In addition, the R-model solutions do not have the large side lobes evident in both the RD-model cross sections and in laboratory experiments involving shoals and unidirectional waves (Berkhoff et al. 1982; Vincent and Briggs 1989). Part of this dis-

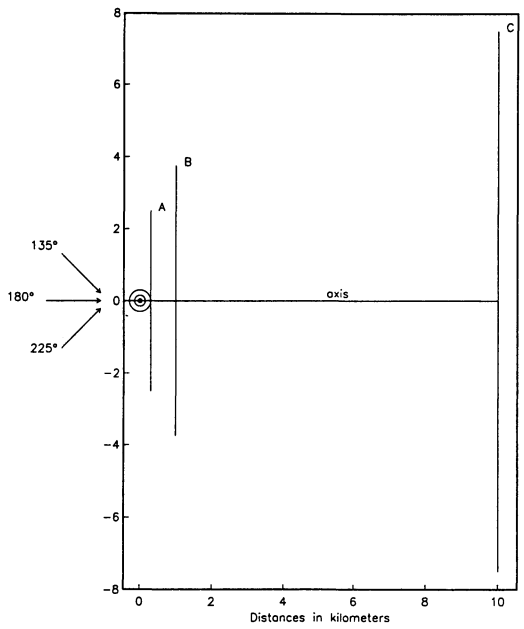

FIG. 4. Locations of Circular Shoal Axis and Cross Sections for Spectral Transformation Comparisons. Cross-sectional Distances from Shoal Center are A = 300 m, B = 1 km, C = 10 km

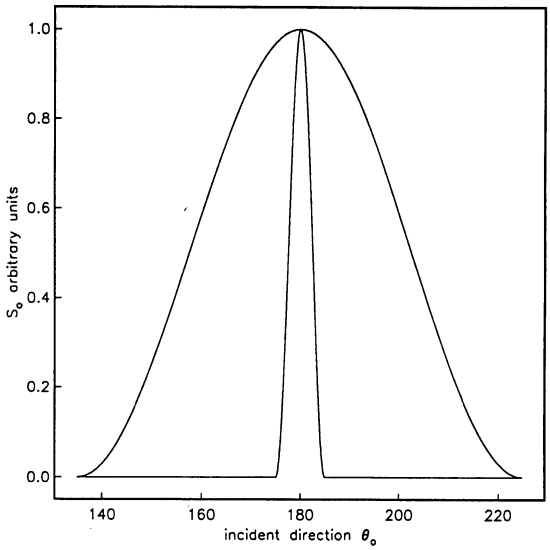

FIG. 5. Narrow and Broad Incident Directional Wave Spectra. Full Width at Half-Maximum (FWHM) = 5° and 45°

crepancy results from a fundamental difference in how the two models view the transformed waves behind the shoal. The R model treats each back-refracted ray as an independent wave train. However, in the case of the circular shoal, three separate rays back-refracted over the center and around opposite sides of the shoal can have the same incident direction, θ_o. For example, this can be seen in Fig. 3, with $\theta_o = 180°$ being associated with three different values of θ. When this incident direction is transformed using Eq. 3, the multiple contributions to the transformed spectrum are treated independently when integrating $S(\omega, \theta)$ to estimate the wave energy. That is, waves from different transformed directions are assumed to have no phase coupling, and standing waves are not possible. This is not the case for the RD model, where multiple transformed wave directions, resulting from a single incident direction, are phased-locked and manifested in the energy estimates as a partially standing wave field. Thus, the present R model does not predict side lobes because the relative phase information of crossing wave trains is not retained.

The spectral transformations of a broad directional spectrum (Fig. 7) resulted in better agreement between the two models. The maximum R-model wave energy immediately behind the shoal was much smaller than in Fig. 6, but still was twice as large as the RD result. The intense focusing of wave energy over the shoal again prevented the R model from being quantitatively accurate in the very near field. However, the improvement in model agreement at cross sections B and C suggests a possible role for the R model in wave energy estimates not directly over the shoal. With a further broadening of the incident spectrum the two model solutions continue to converge, but the solutions behind the shoal become relatively featureless.

The R model overestimates the relative energy maximum in regions of

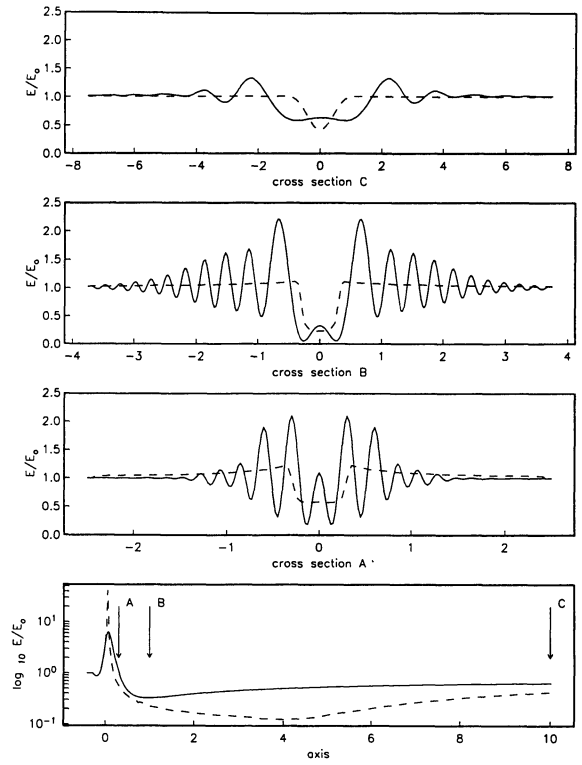

FIG. 6. Normalized, Directionally Integrated Wave Energy for Circular Shoal (Transect Locations Shown in Fig. 4). Narrow Directional Case, FHWM = 5°, Wave Frequency f = 0.06 Hz. Solid and Dashed Lines are RD and R Models, Respectively. Distances in km

strong wave energy convergence and fails to resolve the interference pattern associated with a transformed wave spectrum containing phase-locked directional components. Both of these errors are reduced as the incident directional spectrum becomes broader. The energy maximum is reduced because the caustic point, or the region with the strongest spatial wave energy gradients, shifts with a change in incident direction. Thus, through directional averaging, broader incident spectra produce smoother solutions in these areas, with a larger region of increased energy but a smaller overall relative energy maxima. The lack of phase information in the R model becomes less important, since both models are estimating the transformed energy from a wider directional range of phase-independent incident waves. A complete discussion of spectral refraction-diffraction model solutions behind a shoal can be found in Panchang et al. (1990).

Spectral Transformations over Natural Bathymetry

To address a more practical problem, model solutions are compared for a section of coastline (Mission Beach, California, Fig. 8) chosen for its rel-

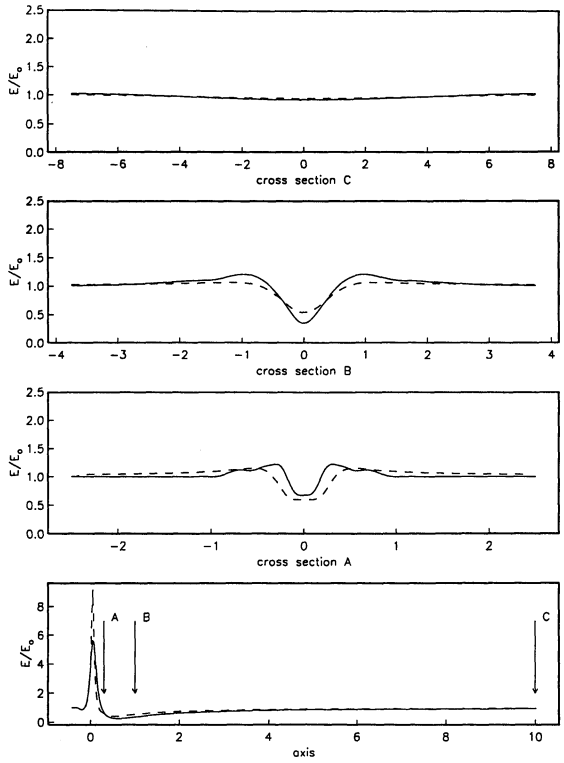

FIG. 7. Normalized, Directionally Integrated Wave Energy for Circular Shoal. Broad Directional Case, FWHM = 45°, Same Format as Fig. 6

atively broad shelf (by West Coast standards) and mild bathymetry. Three cross sections, centered in the grid to minimize the effects of numerical noise generated at the grid boundaries, are used to illustrate the evolution of the solutions from transitional to shallow-water depths. The model wave parameters are the same as those used for the circular shoal. The grid spacing in this case is $x = 78$ m, $y = 92$ m, for the R model, and $x = 26$ m, $y = 23$ m, for the RD model.

Results for the narrow deep-water directional spectrum (Fig. 5) are shown in Fig. 9. Although diffractive effects are usually associated with complicated bathymetries or coastal structures, they also can play an important role on much simpler bathymetries. Even though the bathymetry is smooth, the waves must propagate for some distance over transitional water depths. The R and RD solutions begin to diverge in the intermediate depths (50–100 m) of cross sections A and B, and differ by more than a factor of two in E/E_o at a depth of 10 m. It is interesting to note that the R-model solutions show more spatial structure than the RD solutions. This is quite the opposite of the circular shoal solutions for the narrow spectrum. In this case, the bathymetry is too mild to create the large RD interference patterns that form behind the shoal. Instead the present differences occur because the R model

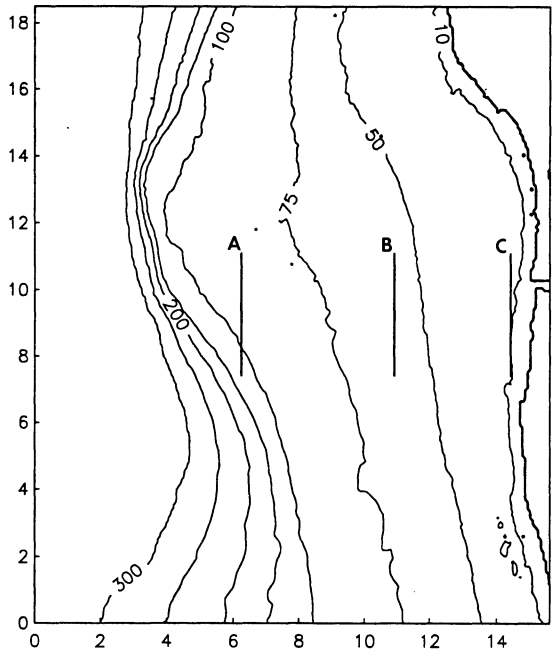

FIG. 8. Bathymetry near Mission Beach, California, and Cross Sections for Model Comparisons. Distances are in km; Depths are in Meters

overestimates wave energy convergence in the near field of mild caustic-producing bathymetry.

The estimates for a broad deep-water directional spectrum (Fig. 10) are in much better agreement. Comparisons at cross sections A and B are nearly identical, although featureless, and the solutions continue to compare well at cross section C. The broad incident spectrum results in slightly smoother RD-model estimates. More importantly, it smooths the R-model solutions in areas of wave energy convergence. The combination of milder bathymetry and a broad incident spectrum minimizes the overall effect of diffraction in this case.

The additional dotted line on cross section C (Figs. 9 and 10) is the RD-model solution for unidirectional waves from 180° (the peak direction of the incident spectrum). With a broad incident spectrum (Fig. 10), the R-model estimates were better (i.e., closer to the spectral RD model) than those of the unidirectional RD model. In this instance, including the directional distribution of wave energy was more important than including diffraction. The opposite is true for a narrow directional spectrum (Fig. 9). These comparisons demonstrate the potential importance of both diffraction and directional wave spreading in transformations over even relatively simple natural bathymetry. We note that the two incident wave directional spectra used in these examples were for illustrative purposes and were not representative of the incident wave spectra typically found in the region.

COMMENTS

The model comparisons demonstrate that the solutions converge with an increase in the incident spectral width and a decrease in the complexity of the bathymetry. As expected, both R and RD solutions become smoother under these circumstances. Why the two models converge toward similar smooth solutions is less clear. Pierson (1951) noted that for caustic-forming bathymetries, the redistribution of wave energy by diffraction is relatively symmetric down wave of the focusing regions. The diffracted wave energy tends to propagate in directions similar in orientation to, but wider than, those of refracted rays that pass through mild caustics. It is this relationship between the two models that results in similar solutions when a broad range of incident directions are contributing to the energy estimate at a given location.

The computational efficiency of the two models is dependent on both the number of locations where transformed wave spectra are needed and on the frequency of the incident waves. The R model transforms wave spectra on a site-by-site basis using back-refraction. The RD model provides solutions over the entire numerical domain. In addition, the acceptable bathymetry grid spacing in the RD model becomes increasingly smaller with higher frequency, shorter wavelength waves. In the R model, the number of numerical calculations grows like $1/\lambda_o$, where λ_o is the incident wavelength. In the RD

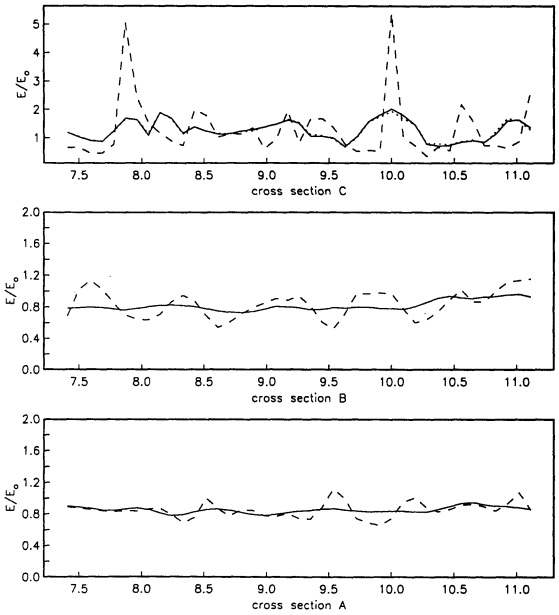

FIG. 9. Normalized, Directionally Integrated Wave Energy for Mission Beach, California. Transect Locations Shown in Fig. 8. Narrow Directional Case, FWHM = 5°, Wave Frequency f = 0.06 Hz. Solid and Dashed Lines are RD and R Models, Respectively. Dotted Line (Upper Panel) is Unidirectional RD. Distances are in km

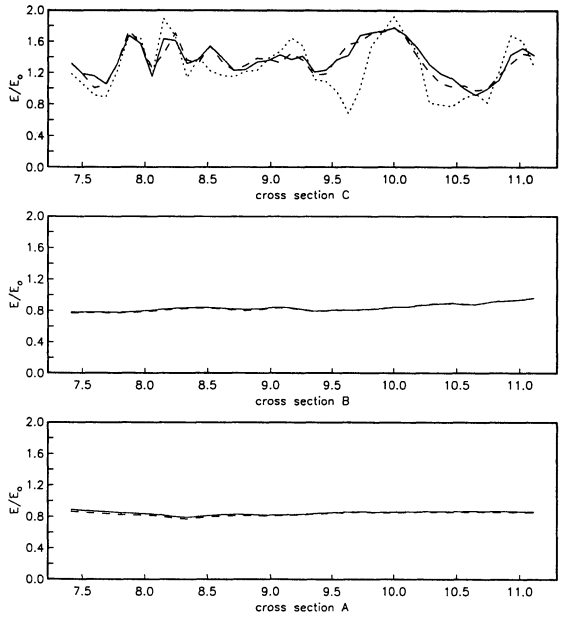

FIG. 10. Normalized, Directionally Integrated Wave Energy for Mission Beach, California. Broad Directional Case, FHWM = 45°. Same Format as Fig. 9

model, the calculations grow like $(1/\lambda_o)^2$. Thus, the R model's efficiency, when compared to RD, increases with both a decrease in the number of estimate locations and an increase in wave frequency. Furthermore, high-frequency, locally generated waves often have broad directional distributions, and the shorter waves undergo milder transformations over a given bottom configuration. The R model is, therefore, most likely to be valid, and has the greatest computational advantage, when modeling local seas. The degree of spectral broadness required for convergence of R and RD solutions depends on the bathymetry and is, therefore, site specific.

Hypothetical directional distributions were used in the previous section to illustrate the importance of the directional spread of incident wave energy in the modeling of finite depth wave transformations. In the laboratory, the incident wave directional distribution is specified a priori and generated using a computer-controlled wave maker [e.g., Vincent and Briggs (1989); Panchang et al. (1990)]. However, field verification of R or RD models requires accurate estimates of naturally occurring incident directional spectra. One potential source of directional wave data is the ubiquitous pitch-and-roll buoy. Unfortunately, the instruments themselves provide a fundamentally low-resolution estimate of wave directionality. Fig. 11 shows two directional distributions, one bimodal and the other unimodal, which both fit the same error-free pitch-and-roll-buoy data exactly [Ochoa and Gonzalez (1990) presents a discussion of the variety of directional spectra that are consistent with the same pitch-and-roll data]. In other words, the two spectra have the same low-order directional moments

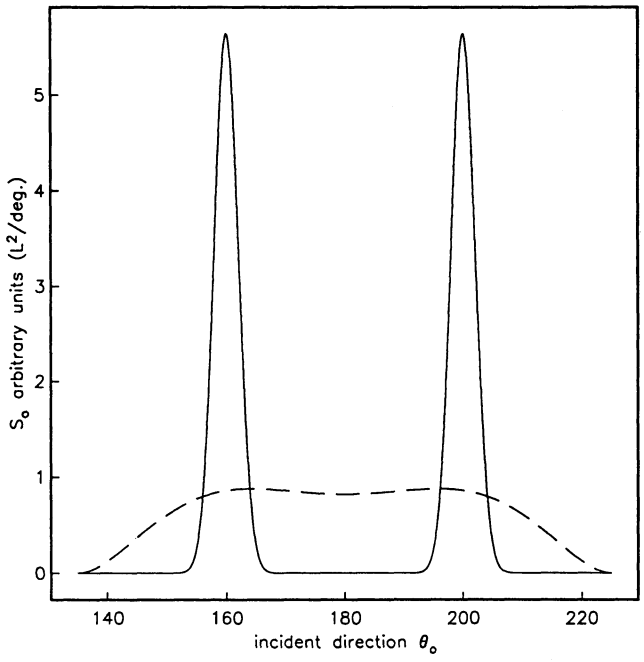

FIG. 11. Bimodal (Solid) and Unimodal (Dash) Directional Spectrum, f = 0.06 Hz. Both Spectra Exactly Fit Same Error-Free Pitch-and-Roll-Buoy Data

$$\int_0^{2\pi} S(\omega,\theta)d\theta \quad \text{and} \quad \left[\int_0^{2\pi} S(\omega,\theta)\sin n\theta d\theta, \int_0^{2\pi} S(\omega,\theta)\cos n\theta d\theta, n = 1,2\right] \ldots\ldots\ldots \quad (5)$$

that form the buoy data. When these two incident spectra are transformed over the bathymetry near Mission Bay using the RD model (Fig. 12), the two solutions differ significantly (a factor of 2 in energy) at the far end of cross section C. The differences are even more significant behind the circular shoal (not shown). Thus, pitch-and-roll data, when used without some additional a priori knowledge of the incident spectrum, may be insufficient for wave-modeling purposes. Further information (e.g., hindcasts or known directional blocking by headlands and islands) can be used with inverse methods to improve buoy directional estimates substantially (Long and Hasselmann 1979; Herbers and Guza 1990), but the buoy may still lack the resolution required to test a propagation model. Accurate estimation of the incident wave spectrum will be a vital component in any field tests of RD models.

Summary

Wave energy estimates from a spectral refraction and a spectral refraction-diffraction model were compared for a circular shoal (Fig. 1) and a relatively mild section of coastal bathymetry at Mission Beach, California (Fig. 8).

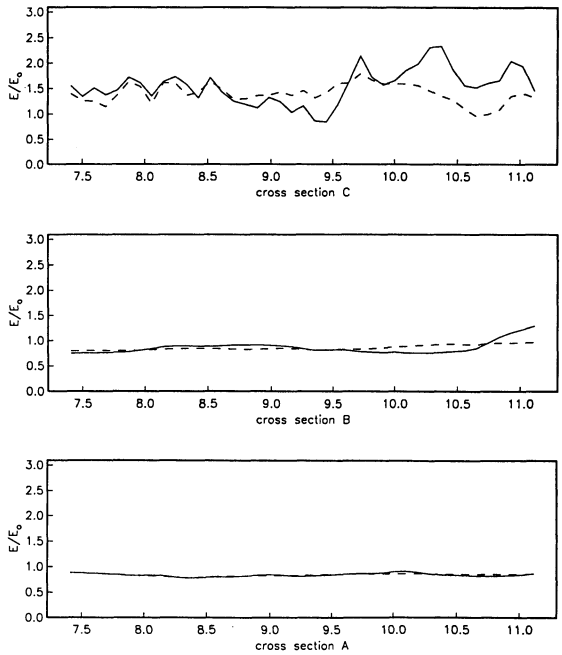

FIG. 12. *RD* **Model Predictions of Normalized, Directionally Integrated Wave Energy (f = 0.06 Hz) for Mission Beach, California. Solid and Dashed Lines are Bimodal and Unimodal Incident Spectra, Respectively (Fig. 11). Distances are in km**

The spectral refraction (backward ray tracing) model, unlike unidirectional (forward ray tracing) models, did not result in infinite or arbitrary wave heights over caustic-producing bathymetries (Fig. 2, 3). However, the R model could not provide quantitatively accurate estimates when the incident directional wave spectrum was narrow (Fig. 6, 9), or the near-field bathymetry was complex (Fig. 6, 7). The R model was a reasonable alternative to the RD model when the incident wave spectrum was broad and the bathymetry was relatively mild (upper panel, Fig. 10), or when the location of interest was in the far field of the complex bathymetry. In the case of a broad incident directional wave spectrum, treating the wave field as a single unidirectional wave produced significant errors in the RD-model predictions with both bathymetries (Fig. 10).

Further, it was illustrated that using pitch-and-roll-buoy directional data alone to specify the incident wave spectrum can lead to a significant degree of uncertainty in the RD-model estimates of transformed wave energy, even over smooth bathymetry (Fig. 12). This conclusion has significant implications for the field verification of RD wave models. Unlike laboratory studies, the incident wave directional spectrum in field experiments is not easily obtained. Therefore, meaningful comparisons between shallow-water field measurements and wave model estimates can be limited by the degree to which the incident wave directional spectrum has been unambiguously resolved.

ACKNOWLEDGMENTS

This research was supported jointly by the California Department of Boating and Waterways, as part of its ongoing wave data applications program, and Sea Grant. Our thanks to Tom Herbers, of the Scripps Institution of Oceanography, who provided the simulated pitch-and-roll-buoy spectra, and Eloi Melo, Universidade Federal do Rio de Janeiro, Brazil, who developed the code for the numerical *RD* model used in this study. In addition, we would like to thank M. Freilich, NASA Jet Propulsion Laboratories, and anonymous reviewers for their critical review of the manuscript.

This work is the result of research sponsored in part by the National Oceanic and Atmospheric Administration, National Sea Grant College Program, Department of Commerce, under grant number NA89AA-D-SG138, project number R/CZ-90, through the California Sea Grant College, and in part by the California State Resources Agency. The U.S. Government is authorized to reproduce and distribute this report for governmental purposes.

APPENDIX. REFERENCES

Berkoff, J. C. W. (1972). Computation of combined refraction-diffraction." *Proc. 13th Coastal Engrg. Conf.*, 471–490.

Berkoff, J. C. W., Booij, N., and Radder, A. C. (1982). "Verification of numerical wave propagation models for simple harmonic linear water waves." *Coast. Engrg.*, 6, 255–279.

Dalrymple, R. A., and Kirby, J. T. (1988). "Models for very wide-angle water waves and wave diffraction." *J. Fluid Mech.*, 192, 33–50.

Dalrymple, R. A., Suh, K. D., Kirby, J. T., and Chae, J. W. (1989). "Models for very wide-angle water waves and wave diffraction. Part 2. Irregular Bathymetry." *J. Fluid Mech.*, 201, 299–322.

Goda, Y. (1985). *Random seas and the design of maritime structures*. University of Tokyo Press, Tokyo, Japan.

Herbers, T. H. C., and Guza, R. T. (1990). "Estimation of wave spectra from multicomponent observations." *J. Phys. Ocean.*, 20(11), 1703–1724.

Isobe, M. (1987). "A parabolic model for transformation of irregular waves due to refraction, diffraction and breaking." *Coast. Engrg. Japan*, 30(1), 33–47.

Izumiya, T., and Horikawa, K. (1987). "On the transformation of directional waves under combined refraction and diffraction." *Coast. Engrg. Japan*, 30(1), 49–65.

Kirby, J. T. (1986a). "Higher-order approximations in the parabolic equation method for water waves." *J. Geophys. Res.*, 91(1), 933–952.

Kirby, J. T. (1986b). "Rational approximations in the parabolic equation method for water waves." *Coast. Engrg.*, 10, 355–378.

Kirby, J. T. (1986c). "Open boundary condition in the parabolic equation method." *J. Wtrwy., Port, Coast., Oc. Engrg.*, 112(3), 460–465.

Kirby, J. T., and Dalrymple, R. A. (1986). "Modeling waves in surfzones and around islands." *J. Wtrwy., Port, Coast., and Oc. Engrg.*, 112(1), 78–92.

LeMehaute, B., and Wang, J. D. (1982). "Wave spectrum changes on a sloped beach." *J. Wtrwy., Port, Coast. and Oc. Engrg.*, 108(1), 33–47.

Long, R. B., and Hasselmann, K. (1979). "A variational technique for extracting directional spectra for multicomponent arrays." *J. Phys. Ocean.*, 9(2), 373–381.

Longuet-Higgins, M. S. (1957). "On the transformation of a continuous spectrum by refraction." *Proc. of the Cambridge Philosophical Society*, 53(1), 226–229.

Ochoa, J., and Gonzalez, O. E. D. (1990). "Pitfalls in the estimation of wind wave directional spectra by variational principles." *Appl. Ocean Res.*, 12(4), 180–187.

Panchang, V. G., Wei, G., Pierce, B. R., and Briggs, M. J. (1990). "Numerical simulation of irregular wave propagation over a shoal." *J. Wtrwy., Port, Coast., and Oc. Engrg.*, 116, 324–340.

Pierson, W. J. (1951). "The interpretation of crossed orthogonals in wave refraction phenomena." *Tech. Memo No. 21,* U.S. Army Corps of Engineers, Beach Erosion Board, Washington, D.C.

Pierson, W. J., Tuttle, J. J., and Wooley, J. A. (1953). "The theory of the refraction of a short-crested Gaussian sea surface with application to the northern New Jersey coast." *Proc. of the Third Conf. on Coastal Engineering,* 86–108.

Radder, A. C. (1979). "On the parabolic equation method for water-wave propagation." *J. Fluid Mech.,* 95, 159–176.

Vincent, C. L., and Briggs, M. J. (1989). "Refraction-diffraction of irregular waves over a mound." *J. Wtrwy., Port, Coast., and Oc. Engrg.,* 115(2), 269–284.